1521-009X/42/9/1485–1492$25.00
Drug Metabolism and Disposition

http://dx.doi.org/10.1124/dmd.114.058008
Drug Metab Dispos 42:1485–1492, September 2014

Effect of CYP2A6 Genetic Polymorphism on the Metabolic Conversion of Tegafur to 5-Fluorouracil and Its Enantioselectivity

Ikuo Yamamiya, Kunihiro Yoshisue, Yuji Ishii, Hideyuki Yamada, and Masato Chiba

Pharmacokinetics Research Laboratories, Taiho Pharmaceutical Co., Ltd., Tsukuba, Japan (I.Y., K.Y., M.C.); and Graduate School of Pharmaceutical Sciences, Kyushu University, Fukuoka, Japan (I.Y., Y.I., H.Y.)

Received March 8, 2014; accepted July 7, 2014

ABSTRACT

Tegafur (FT), a prodrug of 5-fluorouracil, is a chiral molecule, a racemate of *R*- and *S*-isomers, and CYP2A6 plays an important role in the enantioselective metabolism of FT in human liver microsomes (*R*-FT >> *S*-FT). This study examined the enantioselective metabolism of FT by microsomes prepared from Sf9 cells expressing wild-type *CYP2A6* and its variants (*CYP2A6*7*, **8*, **10*, and **11*) that are highly prevalent in the Asian population. We also investigated the metabolism of coumarin and nicotine, both CYP2A6 probe drugs, in these variants. Enzyme kinetic analyses showed that CYP2A6.7 (I471T) and CYP2A6.10 (I471T and R485L) had markedly lower V_{max} values for both enantiomers than wild-type enzyme (CYP2A6.1) and other variant enzymes, whereas K_m values were higher in most of the variant enzymes for both enantiomers than CYP2A6.1. The ratios of V_{max} and K_m values for *R*-FT to corresponding values for *S*-FT (*R*/*S* ratio) were similar among enzymes, indicating little difference in enantioselectivity among the wild-type and variant enzymes. Similarly, both CYP2A6.7 and CYP2A6.10 had markedly lower V_{max} values for coumarin 7-hydroxylase and nicotine *C*-oxidase activities than CYP2A6.1 and other variant enzymes, whereas K_m values were higher in most of the variant enzymes for both activities than CYP2A6.1. In conclusion, the amino acid substitutions in *CYP2A6* variants generally resulted in lower affinity for substrates, while V_{max} values were selectively reduced in CYP2A6.7 and CYP2A6.10. Consistent *R*/*S* ratios among CYP2A6.1 and variant enzymes indicated that the amino acid substitutions had little effect on enantioselectivity in the metabolism of FT.

Introduction

Tegafur (FT) is a prodrug of 5-fluorouracil (5-FU) and has been used for cancer chemotherapy. As shown in Fig. 1, FT is a chiral molecule and contains an asymmetric carbon at the 2′-position of its tetrahydrofuran ring. Our previous study clarified that cytochrome P450 (P450) and thymidine phosphorylase catalyze 5′-hydroxylation and 2′-hydrolysis, respectively, of the tetrahydrofuran ring of FT, followed by sequential decomposition of FT to 5-FU (Yamamiya et al., 2010). Recently we found that CYP2A6 was responsible for the enantioselective metabolism of FT. CYP2A6 catalyzed the conversion of both FT enantiomers to 5-FU most efficiently among P450 isoforms, and the intrinsic clearance of *R*-FT was significantly higher than that of *S*-FT in human liver microsomes (HLMs) (Damle et al., 2001; Yamamiya et al., 2013). Therefore, CYP2A6-dependent enantioselective metabolism likely results in the lower plasma concentrations of *R*-FT than those of *S*-FT in humans after oral administration of tegafur-uracil, a combination drug consisting of racemic FT and uracil at a molar ratio of 4:1 (Damle et al., 2001).

CYP2A6 has been well known as a principal enzyme in the oxidative metabolism of nicotine, followed by sequential conversion to cotinine; however, it has been reported that there are large interindividual and interethnic variations in the cotinine/nicotine ratio in humans after nicotine treatment (Nakajima et al., 1996, 2006; Yamazaki et al., 1999). To date, at least 44 allelic variants of *CYP2A6*, designated as *CYP2A6*2* to **45*, have been identified, 35 of which have mutations in their coding regions, as shown in the Human Cytochrome P450 Allele Nomenclature Database (http://www.cypalleles.ki.se/). Therefore, most of these variations are likely attributed to the genetic polymorphisms in human *CYP2A6* genes. Among these allelic variants, it is known that *CYP2A6*7*, **8*, **10*, and **11* are highly prevalent, with frequencies of 9.8, 1.1, 2.2, and 0.5%, respectively, in the Japanese population (Nakajima et al., 2006). These alleles cause the following amino acid substitutions: I471T (*CYP2A6*7*), R485L (*CYP2A6*8*), R485L and I471T (*CYP2A6*10*), and S224P (*CYP2A6*11*).

Nonsynonymous single nucleotide polymorphisms (SNPs) can change an amino acid sequence of a particular protein, resulting in decreased enzymatic activity and/or stability. Most genetic polymorphisms of *CYP* genes reduce enzymatic activities, and the magnitude of effect depends on the substrate and enantiomers of chiral substrates. For example, CYP2C9 is a major isoform for the hydroxylation of piroxicam and diclofenac. While the *CYP2C9*3* (I359L) variant has drastically reduced piroxicam 5′-hydroxylase activity, diclofenac 4-hydroxylase activity is not affected (Takahashi et al., 2000). There have also been reports that a single amino acid substitution often affects enantioselectivity in the metabolism of chiral substrates. For example, the enantioselectivity between (+)- and (−)-bunitrolol 4-hydroxylase activities is completely reversed by a substitution of methionine at position 374 with valine in the recombinant CYP2D6; V_{max} for (−)-bunitrolol is higher than that for the (+)-isomer in

dx.doi.org/10.1124/dmd.114.058008.

ABBREVIATIONS: CDHP, 5-chloro-2,4-dihydroxypyridine; CL_{int}, intrinsic clearance; CPR, NADPH–cytochrome P450 oxidoreductase; FT, tegafur; 5-FU, 5-fluorouracil; HLM, human liver microsome; IS, internal standard; P450, cytochrome P450; PCR, polymerase chain reaction; SNP, single nucleotide polymorphism; SRS, substrate recognition site.

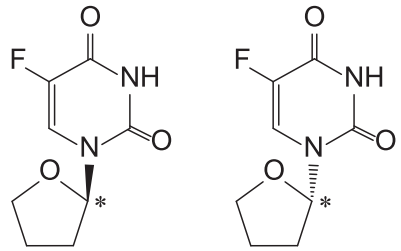

Fig. 1. Chemical structure of FT enantiomers.

the wild-type CYP2D6 enzyme, while the opposite enatioselectivity is observed in the CYP2D6 variant (Narimatsu et al., 1999).

Despite the fact that CYP2A6 is one of major polymorphic isoforms, as described above, the functional impact of its SNPs on the enantioselective metabolism of chiral substrates has not been examined (Fukami et al., 2005; Kimura et al., 2005; Tiong et al., 2010; Han et al., 2012). FT has been approved in several oral formulations for the treatment of various cancers and is thereby one of the most frequently prescribed drugs for cancer chemotherapy in Asia (Watanabe, 2013). Therefore, it is important to examine whether allelic *CYP2A6* variants prevalent in Asia affect kinetics and/or enantioselectivity in the bioactivation of FT to 5-FU.

The aim of this study was to clarify the effects of four genetic variants of *CYP2A6* (*CYP2A6*7*, **8*, **10*, and **11*) on the kinetics of enantioselective conversion of FT to 5-FU. In addition, we characterized the enzyme functions of these variant proteins for coumarin 7-hydroxylase and nicotine *C*-oxidase activities as probes of CYP2A6 function.

Materials and Methods

Chemicals. Human liver cDNA library was purchased from BioChain Institute (Newark, CA). pCRII-TOPO vector, Bac-to-Bac Baculovirus Expression System, pFastBac Dual vector, Cellfectin II, Pluronic F-68, and Grace's Insect Medium were purchased from Life Technologies (Carlsbad, CA). QuikChange Site-Directed Mutagenesis Kit was purchased from Agilent Technologies (Santa Clara, CA). *Taq* DNA polymerase was purchased from Promega (Madison, WI). Rabbit anti-human CYP2A6 polyclonal antibody was purchased from Nosan (Kanagawa, Japan). Rabbit anti-NADPH–cytochrome P450 oxidoreductase (CPR) polyclonal antibody was purchased from Merck KGaA (Darmstadt, Germany). Primers were synthesized at Hokkaido System Science Co. (Hokkaido, Japan). Enantiomers of FT, racemic FT, 5-chloro-2,4-dihydroxypyridine (CDHP), and $^{15}N_2$-5-FU were prepared at Taiho Pharmaceutical Co. (Saitama, Japan). 5-FU, glucose 6-phosphate, acetaminophen, and nicotine were purchased from Sigma-Aldrich (St. Louis, MO). Magnesium chloride hexahydrate, hemin chloride, cotinine, coumarin, propranolol, and 7-hydroxycoumarin were purchased from Wako Pure Chemical Industries (Osaka, Japan). β-NADP$^+$ and glucose-6-phosphate dehydrogenase were purchased from Oriental Yeast Co. (Tokyo, Japan). Other chemicals used were of the highest grade commercially available.

Cells and Tissue Preparations. Sf9 insect cells and *Escherichia coli* DH10Bac Competent Cells were purchased from Life Technologies. Human hepatic cytosol (pooled preparation from 20 donors) was purchased from XenoTech (Lenexa, KS). HLMs (pooled preparation from 150 donors) were purchased from BD Gentest (San Jose, CA). These preparations were stored at −80°C until use.

Isolation of cDNA and Construction of Recombinant Baculoviruses. The open reading frames of human CYP2A6 and CPR were amplified from a human liver cDNA library by means of polymerase chain reaction (PCR) using the following primers: for CYP2A6, forward, 5′-ATGCTGGCCTCAGGGATGCTTCTG-3′, and reverse, 5′-CTACACCATGAGCTTCCTG-3′; and for CPR, forward, 5′-ATGATCAACATGGGAGACTCCCACG-3′, and reverse, 5′-TACTCCCTGGACGTGTGGAGCTAG-3′. *Taq* DNA polymerase was used for the PCR amplification. Each PCR product was ligated into the pCRII-TOPO vector. A mutation was introduced into CYP2A6 cDNA using a QuikChange Site-Directed Mutagenesis Kit according to the manufacturer's instructions. Each pair of complementary mutagenic primers for creation of the mutant variants, *CYP2A6*7*, **8*, **10*, and **11*, is listed in Table 1. The variants carrying a single mutation, i.e., *CYP2A6*7* (I471T), **8* (R485L), and **11* (S224P), were prepared using *CYP2A6*1* (wild-type) cDNA as the template. To prepare the double mutant, *CYP2A6*10*, the SNP region of *CYP2A6*8* was inserted into *CYP2A6*7*. All cDNA clones were sequenced at Hokkaido System Science to verify the entire coding region, including the mutated site. The CYP2A6 and CPR cDNAs were together ligated into a pFastBac Dual vector. Recombinant baculoviruses were constructed using the Bac-to-Bac Baculovirus Expression System according to the manufacturer's instructions. *E. coli* DH10Bac Competent Cells that harbor bacmid vector DNA were transformed with the pFastBac Dual plasmid using the heat shock method. Then the recombinant bacmid DNA was isolated and transfected into Sf9 cells using Cellfectin II–mediated gene transfer to obtain the recombinant baculovirus. Culture supernatants containing the baculovirus were collected, further cultured, and titered by means of the BacPAK qPCR Titration Kit (Takara Bio Inc., Shiga, Japan). The viral preparations (three stocks) that showed a high titer, $>1.3 \times 10^7$ pfu/ml, were used for protein expression. To prepare control microsomes, Sf9 cells were infected with either the empty baculovirus or the virus containing only CPR cDNA.

Expression of CYP2A6 and CPR in Sf9 Cells. Sf9 cells were precultured to a cell density of 1×10^6 cells/ml at 27°C in Grace's Insect Medium containing 10% fetal calf serum and 0.1% Pluronic F-68. The insect cells were then infected with the recombinant virus carrying both CYP2A6 and CPR at a multiplicity of infection of 1.0. A mixture of hemin and albumin was added at 24 hours after infection so that the final concentration of hemin was 2 μg per 215 μg albumin/ml (Grogan et al., 1995). At 72 hours postinfection, the cells were harvested by centrifugation and suspended in 50 mM Tris-HCl (pH 7.4) containing 1.15% KCl and 1 mM EDTA. Insect microsomes were prepared from cellular homogenate by subsequent differential centrifugation steps at 9000*g* for 20 minutes and at 105,000*g* for 60 minutes. After that, the microsomes were reconstituted in 10 mM Tris-HCl (pH 7.4) containing 250 mM sucrose and 0.1 mM EDTA. The protein concentration in the microsomal preparation was measured according to the method of Bradford (1976).

Immunoblotting. Microsomal proteins were heat-inactivated and separated using 12% SDS-PAGE followed by an electrotransfer to a polyvinyldifluoride membrane using an iBlot blotting system (Life Technologies). The membrane was blocked with 5% nonfat skim milk in Tris-buffered saline (pH 7.4) for 1 hour and then soaked in either 5000-fold–diluted rabbit anti-CYP2A6 polyclonal antibody or anti-CPR polyclonal antibody for 1 hour. A goat anti-rabbit IgG antibody conjugated with horseradish peroxidase (Sigma-Aldrich) was used as a secondary antibody for detection. The peroxidase reaction was carried out using ImmunoStar LD (Wako Pure Chemical Industries), and target protein was visualized by an ImageQuant LAS4000 Mini imaging system (GE Healthcare Japan, Tokyo, Japan).

Determination of CYP2A6 and CPR Contents. The CYP2A6 content in insect microsomes was determined according to the quantitative immunoblotting method (Venkatakrishnan et al., 2000). The quantification standard was prepared by serially diluting commercially available recombinant CYP2A6 (BD Gentest). The linearity of CYP2A6 content was confirmed over 100–800 pmol/ml. CPR content was determined as described previously (Fukami et al., 2005).

Assay of 5-FU Formation from FT in Insect Microsomes. As 5-FU formed from FT was subjected to extensive metabolism by dihydropyrimidine dehydrogenase contamination in enzyme preparations, a potent dihydropyrimidine dehydrogenase inhibitor, CDHP, was always added to prevent the unintended loss of 5-FU (Ikeda et al., 2000; Yamamiya et al., 2010, 2013). The reaction mixture (0.1 ml) in the assay of insect microsomal metabolism contained FT, 50–100 pmol/ml CYP2A6, 0.1 mM CDHP, and an NADPH-generating system consisting of 1.3 mM β-NADP$^+$, 3.3 mM glucose 6-phosphate, 3.3 mM magnesium chloride, and 0.4 units of glucose-6-phosphate dehydrogenase in 100 mM Tris-HCl (pH 7.4). The total concentration of microsomal protein was adjusted to 2 mg/ml by adding control microsomes. We ensured that differences in microsomal protein

TABLE 1

Sequences for complementary mutagenic oligonucleotides used in the construction of the indicated variants to generate CYP2A6 variants

The mutated bases are underlined. The double mutations in *CYP2A6*10* were generated by the sequential addition of changes by using oligonucleotides for *CYP2A6*7* and **8*.

Amino Acid Alteration	Allele	Direction	Sequence
I471T	*CYP2A6*7*	Sense	5′-GTCACCTAAGGACAC<u>T</u>GACGTGTCCCCC-3′
		Antisense	5′-GGGGGACACGTCAG<u>T</u>GTCCTTAGGTGAC-3′
R485L	*CYP2A6*8*	Sense	5′-GCCACGATCCCAC<u>T</u>AAACTACACCATGAG-3′
		Antisense	5′-CTCATGGTGTAGT<u>T</u>TAGTGGGATCGTGGC-3′
S224P	*CYP2A6*11*	Sense	5′-CTCTATGAGATGTTC<u>C</u>CTTCGGTGATG-3′
		Antisense	5′-CATCACCGAAG<u>G</u>GAA<u>C</u>ATCTCATAGAG-3′

concentrations between the wild-type and variants did not affect the determinations of kinetic parameters by adjusting the protein concentrations with control microsomes. In some cases, HLMs (1 mg/ml) were used as the enzyme source instead of Sf9 microsomes expressing CYP2A6. The incubation mixture was prewarmed for 5 minutes at 37°C, and then the reaction was started by adding the substrate. The reaction was continued at 37°C for 15–60 minutes and stopped by adding 3 volumes of ice-cold acetonitrile. After centrifugation, the supernatant was collected and stored at −80°C until quantification of 5-FU. Because a small portion of FT is spontaneously converted to 5-FU, the amount of 5-FU formed in the incubation with control microsomes was subtracted from the total yield obtained in the enzymatic reaction. The 5-FU in samples was quantified by means of a previously developed method (Yamamiya et al., 2013).

Assay of Coumarin 7-Hydroxylase and Nicotine *C*-oxidase Activity. In the assay of coumarin 7-hydroxylase activity, the reaction mixture contained coumarin, 10 pmol/ml CYP2A6, and an NADPH-generating system in 100 mM Tris-HCl (pH 7.4). The assay of nicotine *C*-oxidase activity was performed as follows. Because the conversion of nicotine-Δ1′(5′)-iminium ion, which is formed from nicotine by CYP2A6 catalysis, to cotinine requires cytosolic aldehyde oxidase, we added the human hepatic cytosol at a concentration of 3 mg/ml to the reaction mixture. For the assay of coumarin 7-hydroxylase and nicotine *C*-oxidase activities, the total concentration of microsomal protein was adjusted to 0.25 mg/ml by adding control microsomes. In a separate experiment, HLMs (0.25 mg/ml) were used as the enzyme source instead of Sf9 microsomes expressing CYP2A6. After preincubation at 37°C for 5 minutes, the reaction was initiated by adding the substrate, and the mixture was then incubated at 37°C for 10–30 minutes. The reaction was stopped by adding an equal volume of ice-cold acetonitrile containing internal standard (IS) to the reaction mixture, followed by centrifugation. The supernatant was collected and stored at −80°C until analysis.

Concentrations of 7-hydroxycoumarin and cotinine were measured using liquid chromatography–tandem mass spectrometry. The analytical system consisted of an HP 1100 liquid chromatograph (Agilent Technologies) coupled with an API 4000 triple-quadrupole mass spectrometer (AB Sciex, Framingham, MA) equipped with a Turbo V source and electrospray ionization interface. Positive electrospray ionization was used for all metabolites and ISs. Sample separation was performed using a Unison UK-C18 (2.0-mm i.d. × 50 mm, 3 μm; Imtakt, Kyoto, Japan) at a flow rate of 0.2 ml/min of the mobile phase consisting of (A) 0.1% formic acid for the 7-hydroxycoumarin assay or 10 mM formic ammonium for the cotinine assay and (B) acetonitrile at 40°C. The following gradients were used: in the 7-hydroxycoumarin assay, 20 to 95% B in 5 minutes, 95 to 20% B in 0.1 minute, and 20% B held for 5 minutes; and in the cotinine assay, 10 to 70% B in 2 minutes, 70 to 10% B in 0.1 minute, and 10% B held for 4 minutes. The precursor/product ion mass transitions were monitored for determination of the metabolites and ISs: *m/z* 163.0/107.0 for 7-hydroxycoumarin, *m/z* 177.0/98.0 for cotinine, *m/z* 260.0/116.0 for propranolol (IS for 7-hydroxycoumarin), and *m/z* 152.0/110.0 for acetaminophen (IS for cotinine).

Kinetic Analysis. For determining kinetic parameters, FT, coumarin, and nicotine concentrations varied in ranges between 0.03 and 10 mM, 0.1 and 30, and 3 and 500 μM, respectively. All reactions were performed in a linear range of the metabolite formation with respect to enzyme amount and incubation time. Kinetic parameters were estimated by fitting the data to eq. 1 (monophasic kinetics) or eq. 2 (biphasic kinetics):

$$V = V_{max} \times S/(K_m + S) \quad (1)$$

$$V = V_{max1} \times S/(K_{m1} + S) + V_{max2} \times S/(K_{m2} + S) \quad (2)$$

where V is metabolite formation rate; S is substrate concentration in the incubation mixture; K_{m1} and K_{m2} are Michaelis-Menten constants for high- and low-affinity phases, respectively; and V_{max1} and V_{max2} are maximum velocities for high- and low-affinity phases, respectively.

Statistical Analysis. Kinetic parameters ± S.E. of recombinant CYP2A6 and HLM were calculated by fitting the data on the formation rates of metabolites and concentrations of substrates to the Michaelis-Menten equation by nonlinear regression analysis, using Phoenix WinNonlin Professional version 6.1 (Certara, St. Louis, MO). The intrinsic clearance (CL_{int}) was calculated by dividing V_{max} by K_m. Assuming normal distribution as the sample size got larger, statistical comparisons of the Michaelis-Menten parameter estimates between the wild-type and variant enzymes were carried out using the following two-sided test statistic:

$$z = |P_w - P_v| / \sqrt{S.E._w^2 + S.E._v^2} \quad (3)$$

where P_w and $S.E._w$ are the K_m or V_{max} value of the wild-type and the standard error of the kinetic parameter estimate of the wild-type, respectively; and P_v and $S.E._v$ are the K_m or V_{max} value of the variant and the standard error of the kinetic parameter estimate of the variant, respectively. A P value of <0.05 was considered significant.

Results

Expression of CYP2A6 and CPR in Sf9 Cells. The protein expression of CYP2A6 variants and CPR in the microsomes prepared from Sf9 cells was determined by immunoblot analyses after separation by SDS-PAGE (Fig. 2), which were also used to quantify CYP2A6 content in each preparation (Table 2). In this study, the CYP2A6 proteins prepared were named according to the inclusion criteria of the Human Cytochrome P450 Allele Nomenclature Database. The CPR content was calculated from NADPH–cytochrome

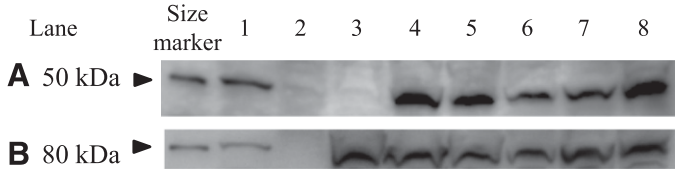

Fig. 2. Immunoblot analyses of variant CYP2A6 (A) and CPR (B) in insect microsomes. Microsomes loaded at 10–20 μg of protein per well were subjected to SDS-PAGE in 12% acrylamide gels and then transferred electrophoretically to a polyvinyldifluoride membrane. The immunoblots were probed with anti-CYP2A6 and anti-CPR antibodies followed by horseradish peroxidase–conjugated goat anti-rabbit antibody. The antigen-antibody complexes were detected using a chemiluminescent assay. The commercially available insect microsomes expressing both CYP2A6 and CPR were loaded onto lane 1 as a positive control. Control Sf9 microsomes expressing neither CYP2A6 nor CPR prepared in this study were loaded onto lane 2. Lanes 3–8 contained the Sf9 microsomes expressing the following enzymes: CPR (3), CYP2A6.1 and CPR (4), CYP2A6.7 and CPR (5); CYP2A6.8 and CPR (6), CYP2A6.10 and CPR (7), and CYP2A6.11 and CPR (8).

TABLE 2

Expressions of CYP2A6 and CPR in insect microsomes expressing wild-type CYP2A6 or its variants

Enzyme (Amino Acid Alteration)	CYP2A6	CPR	CPR/CYP2A6 Ratio
	pmol/mg protein		
CYP2A6.1 (wild-type)	102	21.4	0.22
CYP2A6.7 (I471T)	69.8	15.4	0.22
CYP2A6.8 (R485L)	71.8	17.1	0.24
CYP2A6.10 (I471T and R485L)	59.7	17.4	0.29
CYP2A6.11 (S224P)	130	32.1	0.25

c reductase activity in each preparation by using reported specific activity of microsomal CPR (Table 2). Rabbit anti-CYP2A6 and anti-CPR polyclonal antibodies detected CYP2A6 and CPR expressed in Sf9 cells with molecular masses of approximately 50 and 80 kDa, respectively, which corresponded to known molecular weights of these enzymes (Vermilion and Coon, 1978; Tiong et al., 2010). The molecular weight of the positive control for CYP2A6 (Fig. 2, lane 1) was similar to that of microsomes expressing CYP2A6.1 (Fig. 2, lane 4) or each variant (Fig. 2, lanes 5–8). In contrast, immunoreactivity with anti-CYP2A6 antibody was absent in the control microsomes (Fig. 2, lane 2) and in the microsomes prepared from cells only expressing CPR (Fig. 2, lane 3). The expression content of CYP2A6 (and CPR) and molar ratio of CPR to CYP2A6 in each sample are summarized in Table 2. While the expression contents of CYP2A6 and CPR varied from 59.7 to 130 and from 15.4 to 32.1 pmol/mg of protein, respectively, the molar ratios of CPR to CYP2A6 were similar (0.22–0.29) among microsomal preparations (Table 2).

Kinetic Analyses for Coumarin 7-Hydroxylation and Nicotine *C*-Oxidation. For the functional characterization of CYP2A6 variants, coumarin 7-hydroxylase and nicotine *C*-oxidase activities at different substrate concentrations were fitted to the Michaelis-Menten equation to obtain kinetic parameters in each preparation (Fig. 3, A and B). To assess the validity of the probe assays in the insect microsomes, the kinetic parameters for both reactions in wild-type CYP2A6 (CYP2A6.1) were also compared with those obtained in HLMs. As listed in Table 3, CYP2A6.1 and HLMs had the same K_m values (1.7 μM) for coumarin 7-hydroxylation. Moreover, the K_m value for nicotine *C*-oxidation in CYP2A6.1 (72 μM) was similar to that (61 μM) in the high-affinity component in HLMs. These results indicated that wild-type CYP2A6 (CYP2A6.1) had a catalytic affinity similar to that of the native enzyme in HLMs. The K_m values for coumarin 7-hydroxylation in all CYP2A6 variants (CYP2A6.7, CYP2A6.8, CYP2A6.10, and CYP2A6.11) were 1.4- to 3.2-fold higher than the value in CYP2A6.1, and the V_{max} values in CYP2A6.7 and CYP2A6.10 were significantly lower than that in CYP2A6.1 by 4- and 7-fold, respectively (Table 3). As a result, all mutations in the *CYP2A6* gene resulted in markedly reduced catalytic activity (as expressed by CL_{int} or V_{max}/K_m) for coumarin 7-hydroxylation; the decreases in catalytic activity were especially pronounced in CYP2A6.7 and CYP2A6.10, which were 17 and 4.7%, respectively, of the wild-type activity in CYP2A6.1 (Table 3). Similar decreases in catalytic activity were observed for nicotine *C*-oxidase activity in allelic variant enzymes (Fig. 3B; Table 3); the K_m values were more than 2-fold higher in all CYP2A6 variants than in CYP2A6.1, and the V_{max} values were markedly lower in CYP2A6.7 and CYP2A6.10 than in CYP2A6.1, resulting in mostly impaired catalytic activities. The nicotine *C*-oxidase activity in CYP2A6.7 was 6.4% of the wild-type activity. Similarly, CYP2A6.10 showed the minimal activity, without reaching apparent saturation at the highest concentration of 500 μM; the K_m value estimated by nonlinear regression analysis was 785 $\pm$ 179 μM.

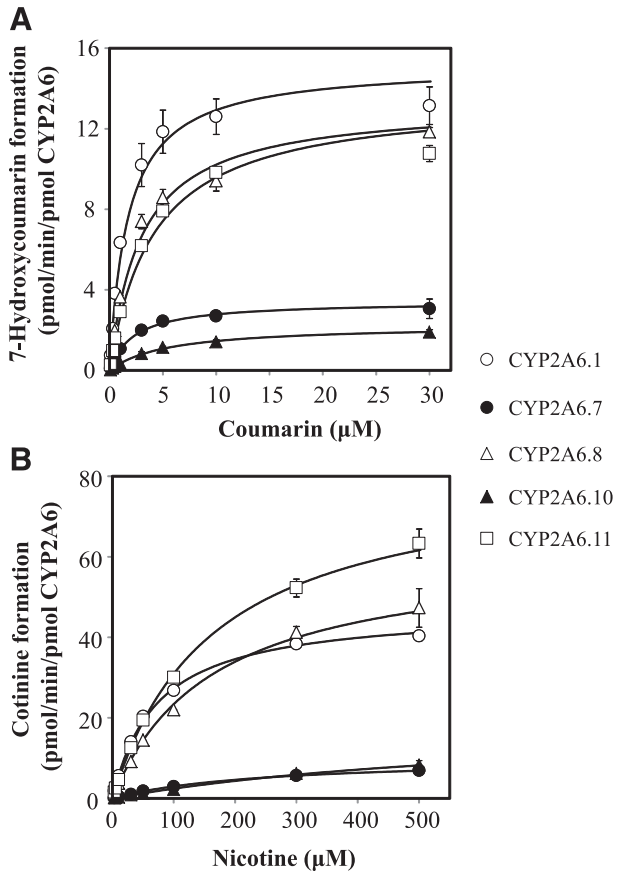

Fig. 3. Michaelis-Menten plots of formation of 7-hydroxycoumrain (A) and cotinine (B) mediated by wild-type CYP2A6 (CYP2A6.1) and its variants. Coumarin (0.1–30 μM) and nicotine (3–500 μM) were incubated with CYP2A6 variants (10 pmol/ml) in the presence of an NADPH-generating system at 37°C for 10–30 minutes. When necessary, the protein concentration was adjusted to 0.25 mg/ml by adding control microsomes. In the assay of nicotine *C*-oxidase, the human hepatic cytosol (final concentration, 3 mg/ml) was also added to the reaction mixture. Kinetic parameters were calculated by curve fitting with the Michaelis-Menten equation, and the results for coumarin 7-hydroxylation and nicotine *C*-oxidation are listed in Table 3. Each data point represents an average of triplicate incubations (mean $\pm$ S.D.) within one experiment.

Kinetic Analyses of Enantioselective Conversion of FT to 5-FU. To examine the effect of *CYP2A6* polymorphisms on enantioselective FT metabolism, the kinetics of 5-FU formations from *R*- and *S*-FT were compared among CYP2A6 variants. The enantioselective conversions from *R*- and *S*-FT to 5-FU catalyzed by CYP2A6 variants were fitted by Michaelis-Menten kinetics (Fig. 4, A and B, respectively), and the obtained kinetic parameters for *R*- and *S*-FT are listed in Table 4. As observed in the kinetics of coumarin 7-hydroxylase and nicotine *C*-oxidase activities in CYP2A6 variants, the K_m values for both conversions of *R*- and *S*-FT to 5-FU were larger in most of the CYP2A6 variants than that in wild-type CYP2A6 (CYP2A6.1), while the V_{max} values for both enantiomers were markedly lower in CYP2A6.7 and CYP2A6.10 than those in CYP2A6.1 and other variants. These alterations resulted in almost completely impaired catalytic activities in CYP2A6.7 and CYP2A6.10: 7.2 and 1.3% of control activity for the metabolism of *R*-FT in CYP2A6.7 and CYP2A6.10, respectively; 7.7 and 0.6% of control activity for the metabolism of *S*-FT in CYP2A6.7 and CYP2A6.10, respectively (Table 4). Although the degree of alterations in kinetic parameters for the metabolism of FT enantiomers differed among the CYP2A6 variants, the ratios of obtained parameters for *R*-FT to those for *S*-FT

TABLE 3

Kinetic parameters for coumarin 7-hydroxylase and nicotine *C*-oxidase activities mediated by wild-type CYP2A6 and its variants

The kinetic parameters were calculated by nonlinear regression analysis. Each kinetic value represents the estimated value ± S.E.

Reaction	Enzyme (Amino Acid Alteration)	Kinetic Parameters			
		V_{max}	K_m	CL_{int}	Fold Change[e]
		pmol/min per pmol CYP2A6	*μM*	*μl/min per pmol CYP2A6*	
Coumarin 7-hydroxylase	CYP2A6.1 (wild-type)	15 ± 1	1.7 ± 0.1	8.7	1.0
	CYP2A6.7 (I471T)	3.4 ± 0.1**	2.3 ± 0.2*	1.5	0.17
	CYP2A6.8 (R485L)	13 ± 1	3.0 ± 0.2**	4.4	0.51
	CYP2A6.10 (I471T and R485L)	2.3 ± 0.1**	5.5 ± 0.5**	0.41	0.047
	CYP2A6.11 (S224P)	14 ± 1	4.2 ± 0.3**	3.2	0.37
	HLMs	611 ± 30[b]	1.7 ± 0.1	365[d]	N.A.
Nicotine *C*-oxidase	CYP2A6.1 (wild-type)	47 ± 1	72 ± 1	0.65	1.0
	CYP2A6.7 (I471T)	10 ± 1**	242 ± 24**	0.041	0.064
	CYP2A6.8 (R485L)	61 ± 2**	161 ± 7**	0.38	0.58
	CYP2A6.10 (I471T and R485L)[a]	N.A.	>500	N.A.	N.A.
	CYP2A6.11 (S224P)	81 ± 1**	163 ± 4**	0.50	0.77
	HLMs	502 ± 14[b]	61 ± 2	8.2[d]	N.A.
		796 ± 105[b]	1.0 ± 0.2[c]	0.78[d]	N.A.

N.A., not available.
[a]CYP2A6.10-mediated formation of cotinine did not reach apparent saturation within the substrate concentration used.
[b]pmol/min per mg protein.
[c]mM.
[d]μl/min per mg protein.
[e]The ratio of CL_{int} (V_{max}/K_m) in each CYP2A6 variant to that in CYP2A6.1.
*$P < 0.05$; **$P < 0.01$ versus wild-type enzyme.

(*R*/*S* ratio in Table 6) were found to be similar among variants, suggesting that the amino acid substitutions in CYP2A6 variants had little effect on enantioselectivity in the metabolism of FT to 5-FU. Furthermore, these amino acid substitutions in CYP2A6 variants reduced the catalytic activity for racemic FT to a similar extent as that for the enantiomers (Fig. 4C; Table 5). Among the reduced catalytic activities for the

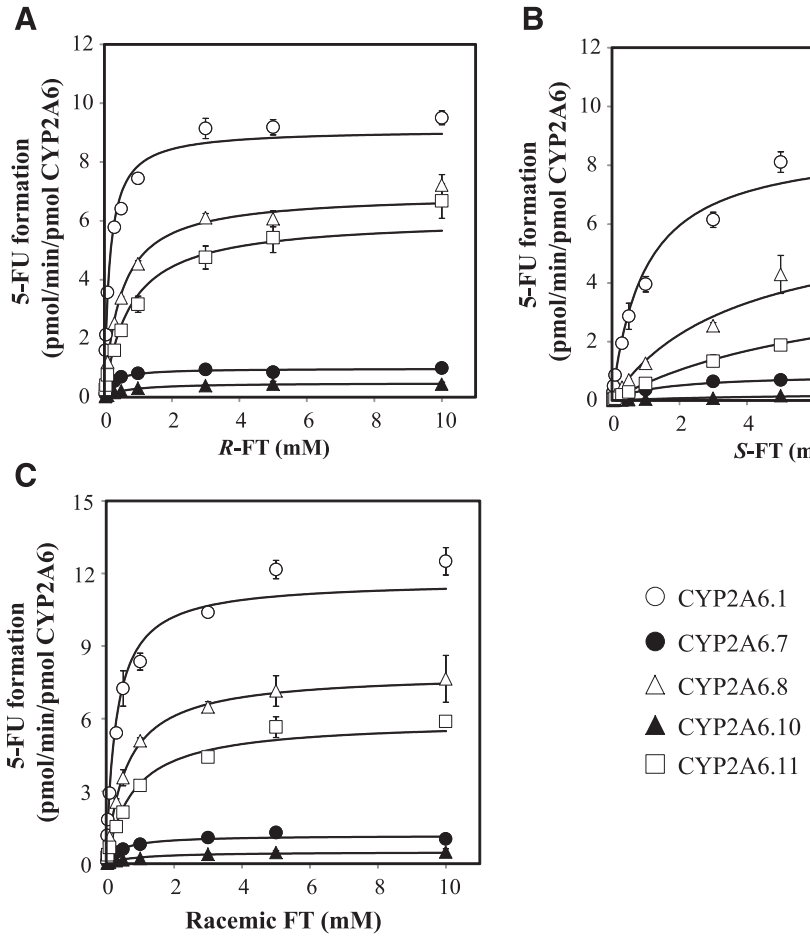

Fig. 4. Michaelis-Menten plots of 5-FU formation from *R*-FT (A), *S*-FT (B), and racemic FT (C) mediated by wild-type CYP2A6 (CYP2A6.1) and its variants. FT (0.03–10 mM) was incubated with CYP2A6 variants (50–100 pmol/ml) and 0.1 mM CDHP in the presence of an NADPH-generating system at 37°C for 15–60 minutes. When necessary, the protein concentration was adjusted to 2 mg/ml by adding control microsomes. Kinetic parameters were calculated by curve fitting with the Michaelis-Menten equation, and the results for the metabolism of *R*- and *S*-FT and of racemic FT are listed in Tables 4 and 5, respectively. Each data point represents an average of triplicate incubations (mean ± S.D.) within one experiment.

TABLE 4

Kinetic parameters for 5-FU formation from *R*- and *S*-FT mediated by wild-type CYP2A6 and its variants

The kinetic parameters were calculated by nonlinear regression analysis. Each kinetic value represents the estimated value ± S.E.

Enantiomer	Enzyme (Amino Acid Alteration)	Kinetic Parameters			
		V_{max}	K_m	CL_{int}	Fold Change[d]
		pmol/min per pmol CYP2A6	*mM*	*nl/min per pmol CYP2A6*	
R-FT	CYP2A6.1 (wild-type)	9.1 ± 0.2	0.16 ± 0.01	58	1.0
	CYP2A6.7 (I471T)	1.0 ± 0.0**	0.23 ± 0.01**	4.2	0.072
	CYP2A6.8 (R485L)	6.9 ± 0.1**	0.48 ± 0.01**	14	0.25
	CYP2A6.10 (I471T and R485L)	0.47 ± 0.02**	0.64 ± 0.03**	0.73	0.013
	CYP2A6.11 (S224P)	6.1 ± 0.3**	0.76 ± 0.05**	8.0	0.14
	HLMs[a]	707 ± 30[b]	0.13 ± 0.01	5.3[c]	N.A.
		439 ± 63[b]	2.0 ± 0.5	0.22[c]	N.A.
S-FT	CYP2A6.1 (wild-type)	9.8 ± 0.4	1.3 ± 0.1	7.7	1.0
	CYP2A6.7 (I471T)	0.88 ± 0.04**	1.5 ± 0.1	0.60	0.077
	CYP2A6.8 (R485L)	6.2 ± 0.4**	3.6 ± 0.3**	1.7	0.23
	CYP2A6.10 (I471T and R485L)	0.31 ± 0.07**	6.6 ± 1.9*	0.046	0.0060
	CYP2A6.11 (S224P)	4.4 ± 0.4**	6.6 ± 0.7**	0.67	0.087
	HLMs	1072 ± 34[b]	1.6 ± 0.1	0.67[c]	N.A.

N.A., not available.
[a]The conversion of *R*-FT to 5-FU followed biphasic kinetics in HLMs.
[b]pmol/min per mg protein.
[c]μl/min per mg protein.
[d]The ratio of CL_{int} (V_{max}/K_m) in each CYP2A6 variant to that in CYP2A6.1.
*$P < 0.05$; **$P < 0.01$ versus wild-type enzyme.

conversion of racemic FT to 5-FU in CYP2A6 variants (Table 5), CYP2A6.7 and CYP2A6.10 had greatly impaired catalytic activities for the metabolism of racemic FT, which were 6.8 and 1.3%, respectively, of control activity in CYP2A6.1. As observed in the metabolism of CYP2A6 probe drugs, CYP2A6.1 had very similar K_m values for the metabolism of *R*- and *S*-FT and racemic FT (0.16, 1.3, and 0.29 mM, respectively) to those of a high-affinity component in HLMs (0.13, 1.6, and 0.27 mM, respectively), which predominantly catalyzes the conversion of FT to 5-FU in HLMs (Tables 4 and 5).

Discussion

The present study established a baculovirus-Sf9 cell system coexpressing CYP2A6 variants and CPR, which allowed the high-level production of active proteins without modifications from full-length P450 cDNAs, and the system was used to analyze the effect of amino acid substitutions in CYP2A6 on the kinetics of enantioselective metabolism of FT in the formation of 5-FU. Microsomes prepared from transfected Sf9 cells had CYP2A6 protein and catalytic activity with comparable CYP2A6/CPR expression level ratios among the variants, suggesting that the wild-type and variant CYP2A6 enzymes were allowed similar access to electrons supplied by CPR (Fig. 2; Table 2).

The enantioselective conversion of FT to 5-FU is exclusively mediated by CYP2A6, and many genetic variants have been identified in the *CYP2A6* gene. Most mutations that have emerged in the *CYP2A6* gene are presumed to cause interindividual and interethnic variations in CYP2A6-dependent metabolism; indeed, the allele frequency of *CYP2A6* polymorphisms is highly variable between ethnic groups. For example, African Americans and white Americans prevalently possess allelic variants including *CYP2A6*2*, **14*, **16*, and **21* alleles, which are not found in the Japanese population (Nakajima et al., 2006). In contrast to American populations, the *CYP2A6*4*, **7*, **8*, **9*, **10*, **11*, **13*, and **15* alleles are known to be prevalent in Asian populations. Of these, *CYP2A6*9*, **13*, and **15* have a SNP in the promoter region that results in decreased CYP2A6 expression, leading to loss of activity (Nakajima et al., 2006). On the

TABLE 5

Kinetic parameters for 5-FU formation from racemic FT mediated by wild-type CYP2A6 and its variants

The kinetic parameters were calculated by nonlinear regression analysis. Each kinetic value represents the estimated value ± S.E.

Recombinant Enzyme (Amino Acid Alteration)	Kinetic Parameters			
	V_{max}	K_m	CL_{int}	Fold Change[d]
	pmol/min per pmol CYP2A6	*mM*	*nl/min per pmol CYP2A6*	
CYP2A6.1 (wild-type)	12 ± 0	0.29 ± 0.01	40	1.0
CYP2A6.7 (I471T)	1.2 ± 0.0**	0.43 ± 0.02**	2.7	0.068
CYP2A6.8 (R485L)	7.8 ± 0.2**	0.58 ± 0.02**	14	0.34
CYP2A6.10 (I471T and R485L)	0.46 ± 0.03**	0.86 ± 0.10**	0.54	0.013
CYP2A6.11 (S224P)	5.9 ± 0.2**	0.79 ± 0.04**	7.5	0.19
HLMs[a]	679 ± 49[b]	0.27 ± 0.02	2.6[c]	N.A.
	786 ± 56[b]	3.7 ± 0.5	0.21[c]	N.A.

N.A., not available.
[a]The conversion of racemic FT to 5-FU followed biphasic kinetics in HLMs.
[b]pmol/min per mg protein.
[c]μl/min per mg protein.
[d]The ratio of CL_{int} (V_{max}/K_m) in each CYP2A6 variant to that in CYP2A6.1.
**$P < 0.01$ versus wild-type enzyme.

other hand, the *CYP2A6*4* allele is a gene deletion type, and its homozygous genotype is associated with a complete absence of enzymatic activity (Nakajima et al., 2004). For example, a positive correlation exists between expression level of CYP2A6 mRNA and coumarin 7-hydroxylase activity in liver samples from Japanese individuals carrying *CYP2A6*1* (wild-type), **4*, or **9* alleles (Yoshida et al., 2003). Because the decreasing effects of *CYP2A6*4* and **9* alleles identified as regulatory polymorphisms on CYP2A6 activity would be independent of substrate recognition and substrates, the kinetic analyses for these alleles were excluded in the present study. For the other allelic variants prevalent in Asian populations (*CYP2A6*7*, **8*, **10*, and **11* alleles), it has been reported that these variants have reduced either in vivo or in vitro metabolic activities of CYP2A6 (Daigo et al., 2002; Fukami et al., 2005; Kimura et al., 2005; Han et al., 2012). The effects of individual SNPs (*CYP2A6*7* and **8*) on the coding region of the *CYP2A6* gene and their combination (*CYP2A6*10*) on enzymatic function or kinetics have not been simultaneously explored in recombinant CYP2A6 enzymes (Fukami et al., 2005; Kimura et al., 2005; Han et al., 2012). Therefore, it was hypothesized that the amino acid substitutions encoded by these allelic variants potentially affect the previously observed enantioselective conversion of FT to 5-FU by altering kinetic parameters for the metabolism by CYP2A6.

A single amino acid change in CYP2A6.7 (I471L) drastically reduced V_{max} values for all CYP2A6-mediated metabolisms tested in the present study, and the decrease was more pronounced in the *CYP2A6*10* allele, which has two amino acid changes (I471L and R485L) (Tables 3 and 4). This observation is consistent with the previous report that nicotine *C*-oxidase activity was markedly reduced in both Japanese and Korean subjects heterozygous for *CYP2A6*7*/*CYP2A6*10* and homozygous for *CYP2A6*7*/*CYP2A6*7* (Yoshida et al., 2002). Both residues of I471 and R485 in CYP2A6 are located in the hinge region close to substrate recognition site (SRS) 6 and responsible for the folding of the protein around this site. Based on the results in this study, they likely have distinct roles in catalysis: comparison of kinetic data among CYP2A6.7 (I471T), CYP2A6.8 (R485L), and CYP2A6.10 (I471T and R485L), variants prevalent in the Asian population, revealed that I471 played a more important role in determining CYP2A6 catalytic capacity (V_{max}) for all CYP2A6 substrates than R485, whose substitution alone had little or no effect on the capacity.

Carbon monoxide difference spectral analysis has demonstrated that the I471T substitution reduces the thermal stability of holoenzyme (Ariyoshi et al., 2001), which is also likely to contribute to the marked reductions in V_{max} of CYP2A6.7 and CYP2A6.10. The replacement of isoleucine with a hydrophobic side chain to a polar amino acid, threonine, caused by the *CYP2A6*7* and **10* alleles might be expected to change the conformation of CYP2A6, resulting in the decrease of heme folding capacity followed by the disordering of the holoprotein structure. On the other hand, the immunoblot analyses in the present study revealed that CYP2A6.7 and CYP2A6.10 retained stable proteins consisting of both apo- and holo- forms in the insect microsomes (Fig. 2; Table 2). Taken together, the results show that it is possible that the inactive apoproteins are partly presented in CYP2A6.7 and CYP2A6.10. However, it is currently unclear which of the catalytic activity, the stability of the holoprotein, or the heme incorporation in the variant CYP2A6 enzymes has a major effect on the V_{max}.

There has been little information on the role of S224, which is located outside the SRS responsible for the maintenance of CYP2A6 conformation. The S224P substitution affected both V_{max} and K_m, suggesting that this residue contributes to both catalytic capacity and substrate affinity of CYP2A6 (Tables 3 and 4). The three-dimensional structure as revealed by X-ray crystallography illustrates that this residue is located adjacent to helix F, which contributes to the formation of the substrate access site in CYP2A6 (Yano et al., 2005). Therefore, this amino acid change could possibly disrupt the access channel of substrates and modify the spatial structure at the putative active site of CYP2A6, leading to the alteration of the kinetic properties. The active-site volume of CYP2A6 is <25% of the volumes calculated for CYP2C8, CYP2C9, and CYP3A4 (Yano et al., 2005). The markedly small volume of the active site in CYP2A6 at least reflects differences in the conformation of the peptide backbone that lead to a relatively low pitch of helices F and G over the top of the active-site cavity as well as tighter packing interactions in the remainder of the molecule. It is therefore likely that an alteration of CYP2A6 structure has a greater effect on the access or binding of substrates responsible for the enzymatic affinity compared with other P450 isoforms.

CYP2A6 polymorphisms by the allelic variants tested in the present study resulted in lower affinity of substrate than wild-type CYP2A6, while the enantioselectivity in the metabolism of FT was almost identical between the wild-type and variants (Tables 4 and 6), and subsequently, the extent of decrease in (or fold change of) catalytic activity (CL_{int}) for racemic FT in each variant (Table 5) was similar to that for each stereoisomer (Table 4). These findings suggest that polymorphic amino acid residues in CYP2A6 tested in the present study are not involved in chiral recognition for the binding of FT enantiomers: these amino acid residues are not located in the SRS (Xu et al., 2002; Zhang et al., 2009), and therefore they are less likely involved in the direct interactions with the substrate.

It has been reported that the plasma concentrations of racemic FT are higher in patients with a variant than those with the wild-type *CYP2A6* allele, suggesting that the oral clearance of FT depends on the *CYP2A6* genotype (Daigo et al., 2002; Fujita et al., 2008; Hirose et al., 2010; Chuah et al., 2011). In addition, the positive correlation between cotinine/nicotine ratio and FT clearance confirmed the importance of CYP2A6 in FT bioactivation, and it has been suggested that the correlation potentially facilitates prediction of individual 5-FU concentrations based on a simple nicotine test (Chuah et al., 2011). The kinetic data on FT metabolism reported in this study strongly support this hypothesis: nearly complete losses in enzymatic activities for the conversion of FT to 5-FU observed in CYP2A6.7 and CYP2A6.10 suggested that the efficacy of FT could be compromised in patients having these polymorphisms (Tables 4 and 5). CYP2A6 is also the principal enzyme responsible for the metabolism of pilocarpine, letrozole, and valproic acid in humans (Di et al., 2009). Moreover, it has been reported that plasma concentrations of these drugs show high interindividual variability and are associated significantly with *CYP2A6* genotypes (Endo et al., 2008; Tan et al., 2010; Desta et al., 2011). Thus, *CYP2A6* polymorphisms can alter the pharmacokinetics of CYP2A6 substrates, resulting in interindividual variations in their plasma exposures, and hence the association between the genetic variants and clinical responses, including the therapeutic and side effects of the drugs metabolized by CYP2A6, needs to be investigated in further studies.

TABLE 6

R/S ratio of kinetic parameters of FT enantiomers

Recombinant Enzyme (Amino Acid Alteration)	*R/S* Ratio		
	V_{max}	K_m	CL_{int}
CYP2A6.1 (wild-type)	0.93	0.12	7.6
CYP2A6.7 (I471T)	1.1	0.16	7.0
CYP2A6.8 (R485L)	1.1	0.13	8.2
CYP2A6.10 (I471T and R485L)	1.5	0.10	16
CYP2A6.11 (S224P)	1.4	0.11	12

In conclusion, the polymorphic *CYP2A6* alleles prevalently observed in the Japanese population (*CYP2A6*7*, **8*, **10*, and **11*) generally resulted in lower affinity for CYP2A6 substrates, while V_{max} values were selectively reduced in CYP2A6.7 (I471L) and CYP2A6.10 (I471L and R485L) for all CYP2A6 substrates. However, *CYP2A6* polymorphisms had the same degree of effect on 5-FU formation from two enantiomers of FT, suggesting that plasma concentrations of these isomers are altered in parallel among patients with variant alleles of *CYP2A6*.

Acknowledgments

The authors thank Ken-ichiro Yoshida (Taiho Pharmaceutical Co.) for helpful comments on the manuscript.

Authorship Contributions

Participated in research design: Yamamiya, Yoshisue, Ishii, Yamada.

Conducted experiments: Yamamiya.

Contributed new reagents or analytic tools: Yamamiya, Yoshisue, Ishii, Yamada.

Performed data analysis: Yamamiya.

Wrote or contributed to the writing of the manuscript: Yamamiya, Yoshisue, Ishii, Yamada, Chiba.

References

Ariyoshi N, Sawamura Y, and Kamataki T (2001) A novel single nucleotide polymorphism altering stability and activity of CYP2a6. *Biochem Biophys Res Commun* **281**:810–814.

Bradford MM (1976) A rapid and sensitive method for the quantitation of microgram quantities of protein utilizing the principle of protein-dye binding. *Anal Biochem* **72**:248–254.

Chuah B, Goh BC, Lee SC, Soong R, Lau F, Mulay M, Dinolfo M, Lim SE, Soo R, and Furuie T, et al. (2011) Comparison of the pharmacokinetics and pharmacodynamics of S-1 between Caucasian and East Asian patients. *Cancer Sci* **102**:478–483.

Daigo S, Takahashi Y, Fujieda M, Ariyoshi N, Yamazaki H, Koizumi W, Tanabe S, Saigenji K, Nagayama S, and Ikeda K, et al. (2002) A novel mutant allele of the CYP2A6 gene (CYP2A6*11) found in a cancer patient who showed poor metabolic phenotype towards tegafur. *Pharmacogenetics* **12**:299–306.

Damle BD, Narasimhan NI, and Kaul S (2001) Stereoselective metabolism and pharmacokinetics of tegafur. *Biopharm Drug Dispos* **22**:45–52.

Desta Z, Kreutz Y, Nguyen AT, Li L, Skaar T, Kamdem LK, Henry NL, Hayes DF, Storniolo AM, and Stearns V, et al. (2011) Plasma letrozole concentrations in postmenopausal women with breast cancer are associated with CYP2A6 genetic variants, body mass index, and age. *Clin Pharmacol Ther* **90**:693–700.

Di YM, Chow VD, Yang LP, and Zhou SF (2009) Structure, function, regulation and polymorphism of human cytochrome P450 2A6. *Curr Drug Metab* **10**:754–780.

Endo T, Nakajima M, Fukami T, Hara Y, Hasunuma T, Yokoi T, and Momose Y (2008) Genetic polymorphisms of CYP2A6 affect the in-vivo pharmacokinetics of pilocarpine. *Pharmacogenet Genomics* **18**:761–772.

Fujita K, Yamamoto W, Endo S, Endo H, Nagashima F, Ichikawa W, Tanaka R, Miya T, Araki K, and Kodama K, et al. (2008) CYP2A6 and the plasma level of 5-chloro-2, 4-dihydroxypyridine are determinants of the pharmacokinetic variability of tegafur and 5-fluorouracil, respectively, in Japanese patients with cancer given S-1. *Cancer Sci* **99**:1049–1054.

Fukami T, Nakajima M, Higashi E, Yamanaka H, Sakai H, McLeod HL, and Yokoi T (2005) Characterization of novel CYP2A6 polymorphic alleles (CYP2A6*18 and CYP2A6*19) that affect enzymatic activity. *Drug Metab Dispos* **33**:1202–1210.

Grogan J, Shou M, Andrusiak EA, Tamura S, Buters JT, Gonzalez FJ, and Korzekwa KR (1995) Cytochrome P450 2A1, 2E1, and 2C9 cDNA-expression by insect cells and partial purification using hydrophobic chromatography. *Biochem Pharmacol* **50**:1509–1515.

Han S, Choi S, Chun YJ, Yun CH, Lee CH, Shin HJ, Na HS, Chung MW, and Kim D (2012) Functional characterization of allelic variants of polymorphic human cytochrome P450 2A6 (CYP2A6*5, *7, *8, *18, *19, and *35). *Biol Pharm Bull* **35**:394–399.

Hirose T, Fujita K, Nishimura K, Ishida H, Yamashita K, Sunakawa Y, Mizuno K, Miwa K, Nagashima F, and Tanigawara Y, et al. (2010) Pharmacokinetics of S-1 and CYP2A6 genotype in Japanese patients with advanced cancer. *Oncol Rep* **24**:529–536.

Ikeda K, Yoshisue K, Matsushima E, Nagayama S, Kobayashi K, Tyson CA, Chiba K, and Kawaguchi Y (2000) Bioactivation of tegafur to 5-fluorouracil is catalyzed by cytochrome P-450 2A6 in human liver microsomes in vitro. *Clin Cancer Res* **6**:4409–4415.

Kimura M, Yamazaki H, Fujieda M, Kiyotani K, Honda G, Saruwatari J, Nakagawa K, Ishizaki T, and Kamataki T (2005) Cyp2a6 is a principal enzyme involved in hydroxylation of 1,7-dimethylxanthine, a main caffeine metabolite, in humans. *Drug Metab Dispos* **33**:1361–1366.

Nakajima M, Fukami T, Yamanaka H, Higashi E, Sakai H, Yoshida R, Kwon JT, McLeod HL, and Yokoi T (2006) Comprehensive evaluation of variability in nicotine metabolism and CYP2A6 polymorphic alleles in four ethnic populations. *Clin Pharmacol Ther* **80**:282–297.

Nakajima M, Yamamoto T, Nunoya K, Yokoi T, Nagashima K, Inoue K, Funae Y, Shimada N, Kamataki T, and Kuroiwa Y (1996) Role of human cytochrome P4502A6 in C-oxidation of nicotine. *Drug Metab Dispos* **24**:1212–1217.

Nakajima M, Yoshida R, Fukami T, McLeod HL, and Yokoi T (2004) Novel human CYP2A6 alleles confound gene deletion analysis. *FEBS Lett* **569**:75–81.

Narimatsu S, Kato R, Horie T, Ono S, Tsutsui M, Yabusaki Y, Ohmori S, Kitada M, Ichioka T, and Shimada N, et al. (1999) Enantioselectivity of bunitrolol 4-hydroxylation is reversed by the change of an amino acid residue from valine to methionine at position 374 of cytochrome P450-2D6. *Chirality* **11**:1–9.

Takanashi K, Tainaka H, Kobayashi K, Yasumori T, Hosakawa M, and Chiba K (2000) CYP2C9 Ile359 and Leu359 variants: enzyme kinetic study with seven substrates. *Pharmacogenetics* **10**:95–104.

Tan L, Yu JT, Sun YP, Ou JR, Song JH, and Yu Y (2010) The influence of cytochrome oxidase CYP2A6, CYP2B6, and CYP2C9 polymorphisms on the plasma concentrations of valproic acid in epileptic patients. *Clin Neurol Neurosurg* **112**:320–323.

Tiong KH, Yiap BC, Tan EL, Ismail R, and Ong CE (2010) Functional characterization of cytochrome P450 2A6 allelic variants CYP2A6*15, CYP2A6*16, CYP2A6*21, and CYP2A6*22. *Drug Metab Dispos* **38**:745–751.

Venkatakrishnan K, von Moltke LL, Court MH, Harmatz JS, Crespi CL, and Greenblatt DJ (2000) Comparison between cytochrome P450 (CYP) content and relative activity approaches to scaling from cDNA-expressed CYPs to human liver microsomes: ratios of accessory proteins as sources of discrepancies between the approaches. *Drug Metab Dispos* **28**:1493–1504.

Vermilion JL and Coon MJ (1978) Purified liver microsomal NADPH-cytochrome P-450 reductase. Spectral characterization of oxidation-reduction states. *J Biol Chem* **253**:2694–2704.

Watanabe T (2013) Evidence produced in Japan: tegafur-based preparations for postoperative chemotherapy in breast cancer. *Breast Cancer* **20**:302–309.

Xu C, Rao YS, Xu B, Hoffmann E, Jones J, Sellers EM, and Tyndale RF (2002) An in vivo pilot study characterizing the new CYP2A6*7, *8, and *10 alleles. *Biochem Biophys Res Commun* **290**:318–324.

Yamamiya I, Yoshisue K, Ishii Y, Yamada H, and Yoshida K (2013) Enantioselectivity in the cytochrome P450-dependent conversion of tegafur to 5-fluorouracil in human liver microsomes. *Pharmacol Res Perspect* **1**:e00009.

Yamamiya I, Yoshisue K, Matsushima E, and Nagayama S (2010) Formation pathways of gamma-butyrolactone from the furan ring of tegafur during its conversion to 5-fluorouracil. *Drug Metab Dispos* **38**:1267–1276.

Yamazaki H, Inoue K, Hashimoto M, and Shimada T (1999) Roles of CYP2A6 and CYP2B6 in nicotine C-oxidation by human liver microsomes. *Arch Toxicol* **73**:65–70.

Yano JK, Hsu MH, Griffin KJ, Stout CD, and Johnson EF (2005) Structures of human microsomal cytochrome P450 2A6 complexed with coumarin and methoxsalen. *Nat Struct Mol Biol* **12**:822–823.

Yoshida R, Nakajima M, Nishimura K, Tokudome S, Kwon JT, and Yokoi T (2003) Effects of polymorphism in promoter region of human CYP2A6 gene (CYP2A6*9) on expression level of messenger ribonucleic acid and enzymatic activity in vivo and in vitro. *Clin Pharmacol Ther* **74**:69–76.

Yoshida R, Nakajima M, Watanabe Y, Kwon JT, and Yokoi T (2002) Genetic polymorphisms in human CYP2A6 gene causing impaired nicotine metabolism. *Br J Clin Pharmacol* **54**:511–517.

Zhang ZG, Liu Y, Guengerich FP, Matse JH, Chen J, and Wu ZL (2009) Identification of amino acid residues involved in 4-chloroindole 3-hydroxylation by cytochrome P450 2A6 using screening of random libraries. *J Biotechnol* **139**:12–18.

Address correspondence to: Ikuo Yamamiya, Pharmacokinetics Research Laboratories, Taiho Pharmaceutical Co., Ltd., 3 Okubo, Tsukuba, Ibaraki 300-2611, Japan. E-mail: i-yamamiya@taiho.co.jp